ResearchGate

See discussions, stats, and author profiles for this publication at: https://www.researchgate.net/publication/255765619

Morphological transition of triblock copolymer cylindrical micelles responding to solvent change

ARTICLE *in* SOFT MATTER · JANUARY 2012

Impact Factor: 4.03 · DOI: 10.1039/C2SM07020K

CITATIONS
6

READS
21

5 AUTHORS, INCLUDING:

Xiaoyu Li
Beijing Institute of Technology
16 PUBLICATIONS **124** CITATIONS
SEE PROFILE

Song Hong
Beijing University of Chemical Technology
31 PUBLICATIONS **308** CITATIONS
SEE PROFILE

Hiroshi Jinnai
Tohoku University
234 PUBLICATIONS **4,217** CITATIONS
SEE PROFILE

Guojun Liu
Queen's University
183 PUBLICATIONS **5,996** CITATIONS
SEE PROFILE

Available from: Hiroshi Jinnai
Retrieved on: 26 January 2016

View Article Online / Journal Homepage / Table of Contents for this issue
Dynamic Article Links

Soft Matter

Cite this: *Soft Matter*, 2012, **8**, 2144

www.rsc.org/softmatter

PAPER

Morphological transition of triblock copolymer cylindrical micelles responding to solvent change

Dehui Han,[a] Xiaoyu Li,[a] Song Hong,[b] Hiroshi Jinnai[b] and Guojun Liu*[a]

Received 21st October 2011, Accepted 23rd November 2011
DOI: 10.1039/c2sm07020k

Reported is the morphological transition of micelles of a BCA triblock copolymer after the solvation medium was changed from one that was selective for B and A to one that was selective for A only. Here B, C, and A denote poly(*tert*-butyl acrylate), poly(2-cinnamoyloxyethyl methacrylate), and the amine-bearing poly(*N*,*N*-dimethylaminoethyl methacrylate) blocks respectively. In methanol, BCA formed cylindrical micelles with the insoluble C block as the core and the soluble A and B blocks as the corona. Adding water reduced the solubility of the B coronal chains. The micellar morphological evolution was followed using transmission electron microscopy (TEM) by analyzing samples, which were taken at different times after water addition to the water volume fractions (f_w) of 2.7% and 10.7%, respectively. Also reported are the stabilized morphologies of the micelles formed in methanol/water mixtures with f_w ranging from 2.9% to 23%.

Published on 04 January 2012. Downloaded by KYUSHU UNIVERSITY on 31/03/2014 01:23:40.

I. Introduction

When subjected to photolysis,[1] a solvent composition change,[2–4] a decrease in polymer concentration,[5–7] or a change in the temperature,[8] pH,[9–12] or ionic strength[13] of the solvation medium, the morphology of block copolymer micelles may mutate. Monitoring these morphological transitions and identifying these new equilibrium micellar morphologies are of fundamental interest because they help improve our understanding of polymer chain motion and block copolymer self-assembly. The study of the structural inversion of diblock copolymer micelles[14–16] and vesicles[11] as well as triblock terpolymer vesicles[9] is also of practical importance because these dynamics are related to the rate of drug release if block copolymer micelles[17] or vesicles[18] are to be used in drug delivery. Furthermore, these dynamics are related to the response rate of sensors made based on stimuli-responsive morphological transitions.[19] Based on these considerations, we initiated a study of the morphological evolution of cylindrical micelles of a triblock terpolymer after the solvation conditions were changed. This paper highlights the results of this study.

The triblock copolymer used was poly(*tert*-butyl acrylate)-*block*-poly(2-cinnamoyloxyethyl methacrylate)-*block*-poly(*N*,*N*-dimethyl methacrylate), abbreviated as PtBA-*b*-PCEMA-*b*-PDMAEMA or BCA.

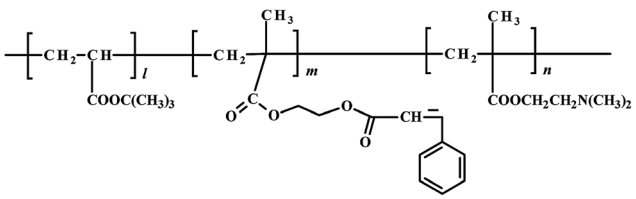

PtBA-*b*-PCEMA-*b*-PDMAEMA

In methanol, BCA formed cylindrical micelles with the insoluble C block making up the core and the soluble B and A blocks forming the corona. The addition of water, which solubilized only the A block, caused the cylindrical micelles to mutate into other morphologies. The morphological evolution was followed by transmission electron microscopic (TEM) analysis of samples taken and aero-sprayed at various times after water addition to f_w = 4.8% and 10.7%. Also analyzed were the micellar morphologies obtained after longer time periods (4 d) after water addition to different f_w's.

While there have been many reports on morphological transitions of block copolymer micelles responding to external perturbations,[1–16] most of the past studies were concerned with the initial and final morphologies of micelles before and after a perturbation was applied. Reports on the use of microscopic techniques for monitoring morphological evolutions are rare. Eisenberg and co-workers used TEM to follow the vesicle to rod conversion and *vice versa*[2,3] as well as sphere to rod[4] conversion and *vice versa*, and proposed mechanisms for these morphological transformations. Fluorescence microscopy was employed by Geng *et al.*[20] to monitor the breakdown of wormlike micelles into spherical micelles. Liu's group has frequently utilized TEM for tracking block copolymer morphological transitions such as the transformation from spherical micelles to flower-like, berry-like, and onion-like micelles[21] as well as the fusion of spherical

[a]*Department of Chemistry, 90 Bader Lane, Kingston, Ontario, Canada K7L 3N6. E-mail: guojun.liu@chem.queensu.ca*
[b]*Institute for Materials Chemistry and Engineering, Kyushu University, 103 Fukuoka Industry-Academia Symphonicity, 203-1 Ohaza Motooka, Nishi-ku, Fukuoka, 819-0385, Japan*

This journal is © The Royal Society of Chemistry 2012

View Article Online

Published on 04 January 2012. Downloaded by KYUSHU UNIVERSITY on 31/03/2014 01:23:40.

micelles into helical micelles[22] and other hierarchical micelles.[23] More recently, Liu and co-workers[24] prepared core–shell–corona cylindrical micelles of a triblock terpolymer with insoluble core- and shell-forming blocks. Upon addition of a solvent that solubilized both the corona and core blocks, the micelles ruptured and transformed into cylinders with twisted sections. TEM was used to monitor the rupture and evolution of the original cylinders, and a mechanism was proposed for this morphological transformation. In this paper, we report results of the reverse experiment, in which the solvent was changed from one that solubilized both terminal blocks of a triblock terpolymer to one that solubilized only one terminal block.

II. Results and discussion

Cylindrical micelles in methanol

As mentioned in the Experimental section, the precursor to BCA was prepared by anionic polymerization, and the polymer thus had a low polydispersity. The repeat unit numbers and weight fractions of the B, C, and A blocks were 160 and 29%, 135 and 50%, as well as 95 and 21%, respectively. Using the literature densities of 1.02, 1.25, and 1.32 g cm^{-3} for the B,[25] C,[25] and A[26] blocks, respectively, we calculated volume fractions of 34%, 47%, and 19% for the three blocks.

Methanol is a selective solvent for B and A. Stirring the polymer in methanol at room temperature between 4 and 7 d yielded BCA cylindrical micelles. Fig. 1a shows a TEM image of the cylindrical micelles after they were sprayed from methanol and stained by OsO_4. A micellar solution was also photolyzed by UV light to crosslink the C domain of the micelles.[27,28] The A block of the structurally locked micelles was then quaternized by reaction with methyl iodide.[29] Fig. 1b shows a TEM image of such a derivatized micellar sample after it was sprayed from *N*,*N*-dimethylformamide.

As mentioned in the literature,[30] the morphologies of block copolymer micelles can change if sufficient time is allowed to evaporate the solvent during TEM specimen preparation. Therefore, different specimen preparation protocols are frequently used to ensure the reproducibility of one's results.[31] Our TEM and AFM specimens were collected by swiftly passing a cellulose-covered TEM grid or a silicon wafer no more than twice through an atomized spray that was generated by a home-built device.[21] Since the sprayed droplets were fine and the distance between the spraying nozzle and the TEM grid or silicon wafer was at least two feet, the methanol solvent had mostly evaporated before the micellar particles landed on the grid or wafer. Thus, we doubt that our micellar particles were able to change their morphology during specimen preparation. However, we do not rule out particle deformation involving intra-particle chain motion either during specimen preparation or specimen storage. For example, the soluble coronal chains could contract inwardly responding to solvent evaporation during their flight from the nozzle to the grid or wafer surface. Alternatively, they may spread on a substrate surface due to favorable polymer/substrate interactions when they are plasticized by residual solvent. Even the insoluble core blocks could deform somewhat during specimen storage due to polymer creeping under gravitation. To minimize specimen mutation, our samples were analyzed by TEM immediately, typically within hours, after they were prepared.

Fig. 1b shows a TEM image of a core-crosslinked micellar sample, whose morphology should not have changed during specimen preparation or sample storage. The fact that cylinders were seen not only in Fig. 1b but also in Fig. 1a suggested that our TEM specimen preparation protocol did not change the morphology of the non-crosslinked micelles.

The cylinders of Fig. 1a were uniformly dark because they were stained with OsO_4, which selectively stained the double bonds of the C core. Meanwhile, the cylinders in Fig. 1b had a core–shell structure, because they were stained with methyl iodide, which stained the coronal A chains. Despite the different appearances, the dark cylinders in Fig. 1a had a diameter of 18 ± 3 nm, which was similar to that of the light cores of the core–shell cylinders in Fig. 1b. This size agreement helped confirm the above structural assignment.

The cylinder shells appeared uniformly gray in Fig. 1b, suggesting that the soluble A and B chains did not undergo significant phase separation in the corona. This might be due to their low repeat unit numbers and thus their compatibility in the solvated state.

Fig. 2 shows an AFM topography and a phase image of the cylindrical micelles after they were sprayed from methanol onto a silicon wafer. No sizable phase segregation was seen between B and A blocks in Fig. 2b. This was consistent with the TEM image shown in Fig. 1b.

The average height for the cylinders was 20 ± 2 nm. Assuming respective volume fractions of 34%, 47%, and 19% for the B, C, and A blocks and that the TEM core diameter of 18 ± 3 nm was similar to that of the C core, while also assuming that the coronal B and A chains shrank to form a dense layer around the C core,

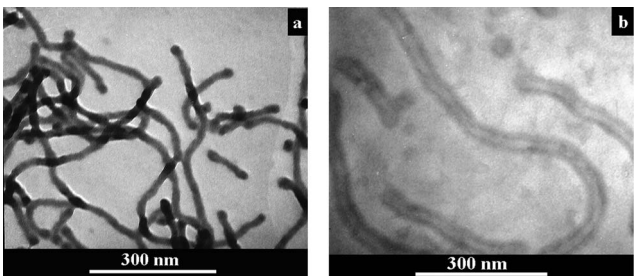

Fig. 1 TEM images of BCA cylindrical micelles sprayed from methanol and stained by OsO_4 (a) and methyl iodide (b).

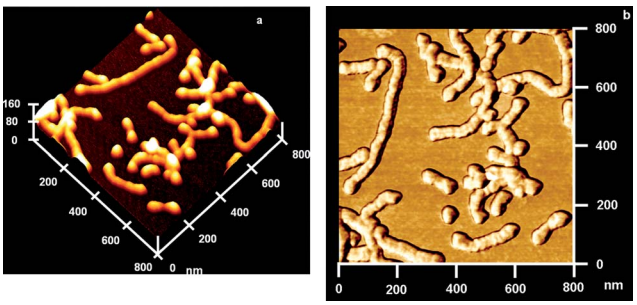

Fig. 2 AFM topography (a) and phase (b) images of BCA cylindrical micelles sprayed onto a silicon wafer from methanol.

View Article Online

Published on 04 January 2012. Downloaded by KYUSHU UNIVERSITY on 31/03/2014 01:23:40.

we calculated a diameter of 26 ± 4 nm for the entire cylinder. This was larger than the value of 20 ± 2 nm determined by AFM. One very likely contributing factor to this discrepancy was that the solvated coronal chains did not actually form a compact layer around the C cylinder. Rather, they became spread out along the surface of the silicon wafer due to favorable interactions with the wafer's surface. In addition, the core cylinders could have become flattened somewhat during AFM specimen preparation and storage.

Micelles in methanol/water

We determined experimentally that the addition of 5.7 vol% of water into a methanol solution of a poly(*tert*-butyl acrylate) homopolymer with 130 repeat units turned the solution cloudy, indicating that the polymer had turned insoluble. The B block of our BCA copolymer was longer, at 160 units. Despite this difference, we designate the B block as "less soluble" and "insoluble" in methanol/water mixtures with f_w < 5.7% and >5.7%, respectively.

Water was added into BCA solutions in MeOH to f_w values of 2.9%, 4.8%, 7.4%, 10.7%, 16.7%, and 23%. The resultant mixtures were subsequently equilibrated for 4 d. Fig. 3 shows TEM images of samples sprayed from such mixtures and then stained with OsO_4.

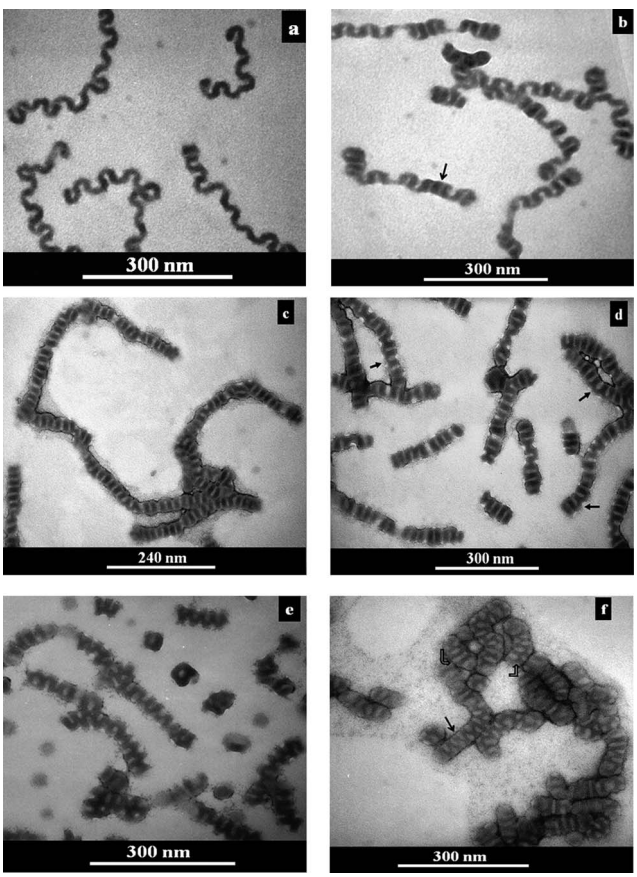

Fig. 3 TEM images of BCA micelles sprayed from methanol/water 4 d after water addition to f_w = 2.9% (a), 4.8% (b), 7.4% (c), 10.7% (d), 16.7% (e), and 23% (f). The samples were stained with OsO_4.

Evidently, water addition transformed the wormlike cylinders of Fig. 1 to other cylindrical structures. At f_w = 2.9%, wriggling cylinders with local folds were formed (Fig. 3a). The diameter of the dark wriggling C cylinders was 17 ± 3 nm, which was the same as the original C cylinders before water addition. The folds visible in Fig. 3b became tighter at f_w = 4.8%. Also, segregated cylinder sections consisting of poorly resolved alternating dark and gray layers (one example is marked by an arrow) were also seen. At f_w = 7.4%, the cylinders visible in Fig. 3c apparently consisted mostly of segmented sections and the contrast between the dark and gray layers improved. Aside from segmented sections, sections consisting of "horseshoes", three examples are marked by arrows, were also seen for micelles prepared at f_w = 10.8% in Fig. 3d. At f_w = 16.7%, mostly horseshoe-shaped sections made up the cylinders shown in Fig. 3e. At f_w = 23%, the cylinder cores in Fig. 3f became substantially thicker and the dark C block formed domains of different shapes, including zigzag sections (one example is marked by a regular arrow), segmented sections (one example is marked by a curved arrow), and network sections (one example is marked by a rectangular arrow).

Fig. 4 shows the AFM topography images of samples sprayed from solutions at f_w = 2.9% and 10.7%. The wriggling structure and segmented sections observed by TEM were confirmed by AFM. Aside from the segmented structures (one example is marked by an end-tagged arrow in Fig. 4b), some horseshoes as marked by regular arrows are also seen in Fig. 4b.

Scheme 1 depicts our interpretation of the chain packing of a wriggling cylinder, a segmented section, and a horseshoe section. The cylinders became wriggled at f_w = 2.9% because the bending of the cylinders facilitated the clustering of the less soluble B chains. According to Scheme 1a, the less soluble B chains became clustered on the concave side of the wriggling C cylinders whilst the soluble A chains stretched into the solvent phase from the convex side of the C cylinders.

At f_w = 4.8%, the B chains became less soluble, the solvent content inside the B-rich phase decreased, and the folds tightened. To confirm the chain packing motif illustrated in Scheme 1a, we photocrosslinked the cylindrical micelles prepared at f_w = 4.8% and then hydrolyzed the B chains to poly(acrylic acid) or PAA. Since the PAA and A chains formed a polyelectrolyte complex, the resultant triblock nanofibers aggregated with each other and were not very dispersible. Despite this, we obtained TEM images of some smaller aggregates after they were aero-sprayed and stained by $UO_2(Ac)_2$, which selectively stained the PAA domains. Fig. 5 shows a TEM image of such a sample and

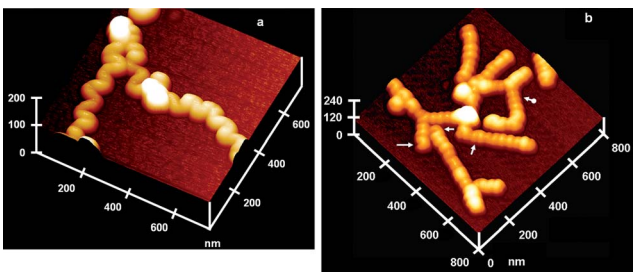

Fig. 4 AFM topography image of BCA cylinders sprayed onto a silicon wafer surface 4 d after water addition to f_w = 2.9% (a) and 10.7% (b).

 This journal is © The Royal Society of Chemistry 2012

View Article Online

Published on 04 January 2012. Downloaded by KYUSHU UNIVERSITY on 31/03/2014 01:23:40.

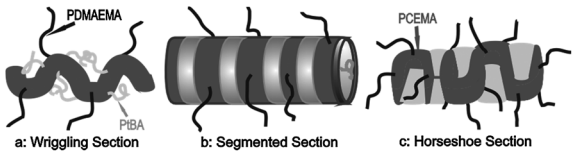

Scheme 1 Illustration of chain packing in wriggling (a), segmented (b), and horseshoe (c) sections.

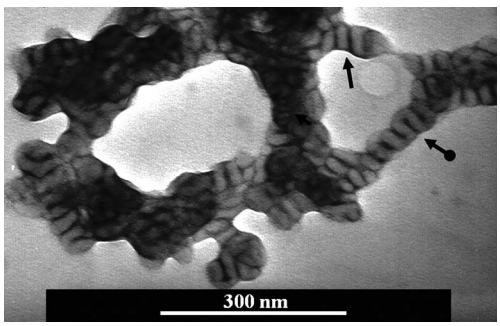

Fig. 5 TEM image of a BCA micellar sample after crosslinking of the C block, hydrolysis of the B block, and staining by $UO_2(Ac)_2$. The micelles were prepared in a methanol/water mixture 4 d after water addition to $f_w = 4.8\%$.

a wriggling section is marked by an end-tagged arrow. The darkly stained PAA chains were indeed concentrated on the concave side of the folded cylinder.

Fold tightening was accompanied by a bending energy increase for the C cylinders. This energy increase destabilized the wriggling cylinders and eventually caused the formation of segmented cylinders, in which the A and C blocks formed alternating disks as illustrated in Scheme 1b. A segmented section was also seen and marked in Fig. 5. A comparison between Fig. 3c, where the C domain was stained with OsO_4, and Fig. 5, where PAA was stained with $UO_2(Ac)_2$, confirmed that the B and C blocks indeed formed the alternating disks. Our statistical analysis yielded average thicknesses of 10 ± 2 and 7 ± 2 nm, respectively, for the C and B disks shown in Fig. 3c. These values were reasonable when considering that the volume fractions were 47% and 34% for the two blocks.

One segmented section is marked by an end-tagged arrow in Fig. 4b, and the segmented sections clearly appear cylindrical. The banded texture likely arose because of the accumulation of the A chains onto the C surfaces. This preferential concentration of the A chains on the C surface was reasonable because A was covalently attached to C and not to B.

While we have used energetic arguments to justify the formation of the wriggling and segmented cylinders, we had no intention to imply that these were the most favored aggregates. Because of the slow motion of polymer chains, particularly at high f_w's such as at 16.7% and 23%, the structures that we observed were probably those that could be achieved within kinetic constraints.[32,33] On an energy map, these would represent structures possessing local energy minima.

Judging from the TEM images alone, we had tremendous difficulty in deciding if the horseshoe-shaped structures were helical. This prompted us to initiate a TEM tomography study.

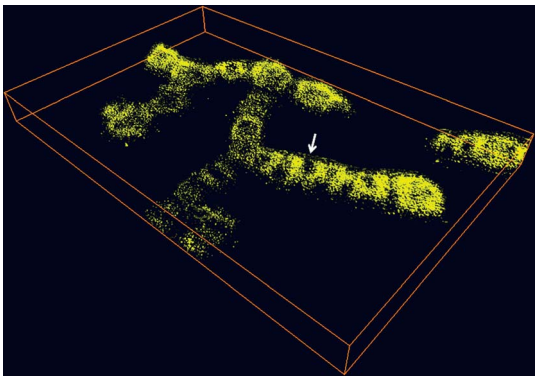

Fig. 6 TEM tomography image of a BCA micellar sample sprayed 4 d after water addition to $f_w = 16.7\%$. The frame volume is $500 \times 320 \times 40\ nm^3$.

Fig. 6 shows a TEM tomography image of several cylinders sprayed from a $f_w = 10.7\%$ solvent mixture. The C domains of the marked cylinder section clearly consisted of fused horseshoes rather than a helix. Also, the shoes clearly had different spatial orientations rather than a 2-D arrangement. Three horseshoes are also marked by regular arrows in Fig. 4b.

The segregation patterns of the C block varied from section to section and from cylinder to cylinder at $f_w = 23\%$. We suspect that this morphological diversity most likely had its roots in the kinetic control of the morphologies.[32,33] The core diameter thickened to 45 ± 6 nm at $f_w = 23\%$ because the interfacial tension between water and the B and C cores increased and these meta-stable species decreased their interfacial energy by increasing the diameter of the core cylinders and decreasing the total interfacial area.

Morphological evolution at $f_w = 2.9\%$

To monitor the morphological transitions of the cylindrical micelles formed in methanol after water addition, we analyzed, by TEM, samples sprayed at different times after water addition to $f_w = 2.9\%$ and $f_w = 10.7\%$. Fig. 7 shows TEM images of samples sprayed at different times after water addition to $f_w = 2.9\%$. The samples were stained with OsO_4.

Fig. 7a–f reveal a number of features. Firstly, no obvious difference was seen between the cylinders that were sprayed 4 min after water addition and those observed in Fig. 1a before water addition. With time, the number of kinks per cylinder increased. This trend suggested that the morphological transition occurred rather slowly, *e.g.* over hours, which was much longer than the time required for solvent evaporation during TEM specimen preparation. Secondly, no obvious cylinder fragmentation was observed throughout the morphological transition. Thirdly, abnormally fat cylinders were seen at $t = 20$ min, 1 h, and 8 h, and some examples of these cylinders are marked by arrows.

As mentioned earlier, the kinks had developed because of the favorable clustering of the less soluble B chains along the cylinder axis. While we do not have sufficient evidence to conclude about the mechanism(s) for this surface chain rearrangement, we will point out the possible mechanisms for this behavior below and indicate which mechanisms we believe are most likely to occur.

Mechanism 1 involves the exchange of polymer chains between the cylindrical micelles and the unimer pool. In methanol

View Article Online

Published on 04 January 2012. Downloaded by KYUSHU UNIVERSITY on 31/03/2014 01:23:40.

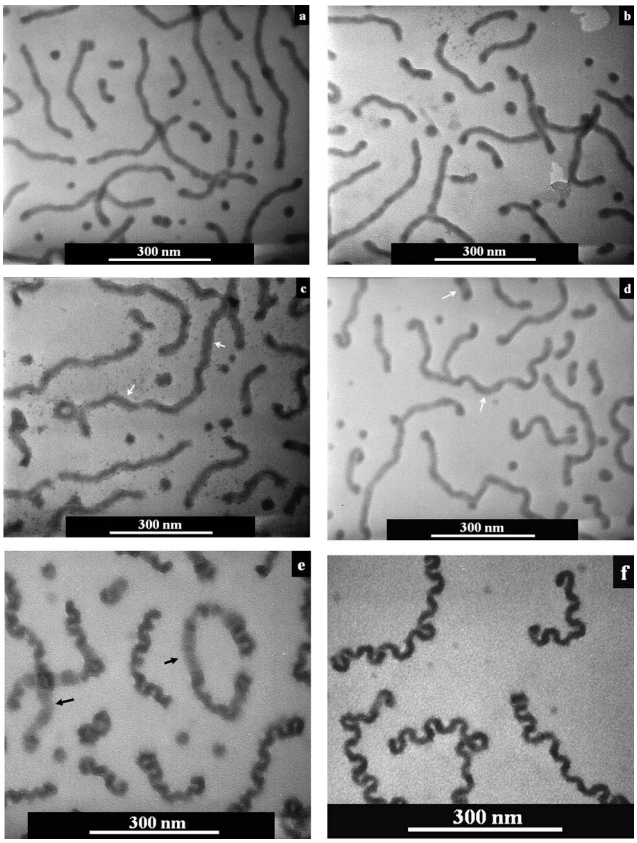

Fig. 7 TEM images of BCA cylinders sprayed 4 min (a), 10 min (b), 20 min (c), 1 h (d), 8 h (e), and 4 d (f) after water addition to $f_w = 2.9\%$.

containing water, the C chains are highly insoluble and thus the critical micelle concentration should be very low. According to Eisenberg[9] and Bates,[32] this mechanism should play a minor role under such circumstances. Aside from the low cmc, one should further realize the challenges associated with extracting a BCA chain, with soluble B and A termini, from a micelle and re-inserting it into another micelle.

Mechanism 2 may involve the fragmentation of the cylindrical micelles into various sections, the rearrangement of the coronal chains in these fragments, and the reassembly of the fragments into kinked cylinders. While we cannot rule out this mechanism, we doubt that this was dominant because we did not see a large population of fragmented cylinders at any of our observation times.

Intra-cylinder chain position shuffling is assumed to occur in mechanism 3. Scheme 2 illustrates two possible pathways for moving a B, or PtBA, chain from an initial diagonal position relative to the A, or PDMAEMA, chain (image a in Scheme 2) to a right-angled position (c). While the scheme is presented in 2-D, one should realize that the actual events occur in a 3-D space and thus the chains are not confined to a 2-D plane.

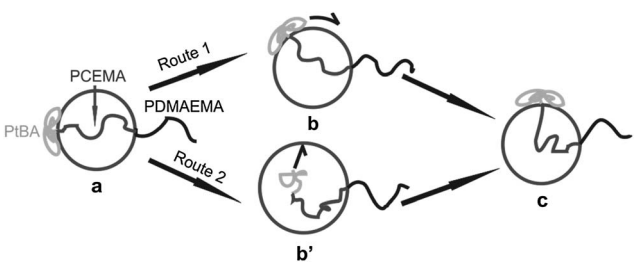

Scheme 2 2-D illustration of two possible routes for coronal chain position shuffling.

Evidently, the B chain migrates because different B chains want to aggregate. Since the coronal chains are solvated, their mobility should be high. The rate limiting step would be chain diffusion or reptation in the C cores. One possible way to attain this surface chain position shuffling is for the C chain in the cylinder core to bend and cut across the C cylinder. Another route is for the B chain to retract into the C core. This leads to the creation of a larger and mixed B and C core. The gradual reptation of this B chain out of this mixed core and its emergence at a perpendicular angle lead to the desired surface chain position.

While we tend to believe that route 1 of mechanism 3 would be more facile than route 2, we cannot rule out the occurrence of route 2. In discussing the inversion of terpolymer triblock vesicles with the middle block forming the vesicle wall, Liu and Eisenberg[9] suggested the possibility of route 2. The fuzzy and fat structures seen in Fig. 7c and d, and particularly in Fig. 7e also suggest the possible occurrence of this route. Despite this evidence, further experiments will be required to confirm the occurrence of this pathway.

Morphological evolution at $f_w = 10.7\%$

The TEM images of samples sprayed from a solution at $f_w = 10.7\%$ at different times after water addition are shown in Fig. 8.

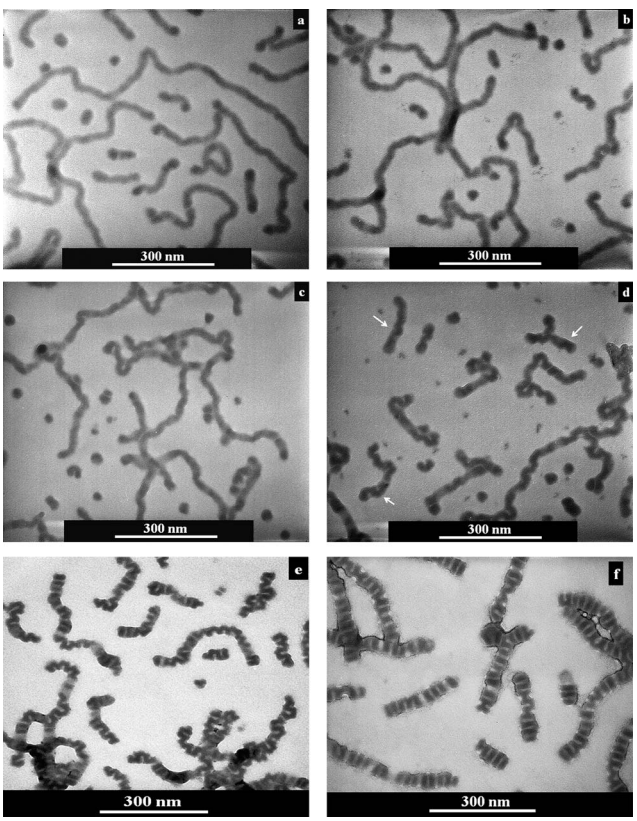

Fig. 8 TEM images of BCA cylinders sprayed 10 s (a), 60 s (b), 5 min (c), 30 min (d), 4 h (e), and 4 d (f) after water addition to $f_w = 10.7\%$.

This journal is © The Royal Society of Chemistry 2012

View Article Online

Published on 04 January 2012. Downloaded by KYUSHU UNIVERSITY on 31/03/2014 01:23:40.

A close examination of the images revealed the following features. Firstly, folding occurred much more quickly than at f_w = 2.7% and many bends due to cylinder folding were already visible at t = 60 s. Secondly, cylinder folding was not the sole mechanism for bend formation. Judging from the three marked fuzzy intermediates shown in Fig. 8d, one may speculate that the bend-like structures could form through the concerted contraction of the original cylinder along the axial direction and the lateral movement of the B and C chains towards different sides. Also, an abnormally large number of small fragments are seen in Fig. 8b–d. Thus, one cannot rule out the fragmentation and recombination mechanism mentioned above. Thirdly, some of the C bends eventually fragmented and contracted to yield segmented cylindrical sections, with some of these bends remaining as structures that we have previously described as horseshoes.

The faster cylinder folding observed at f_w = 10.7% should not be surprising, because B had become completely insoluble at this solvent composition and the attractive force between the B chains had increased relative to that occurring at f_w = 2.7%. However, more studies will be required to gain a better understanding of the morphological transition observed under these conditions.

III. Conclusions

BCA formed cylindrical micelles in methanol. While the insoluble C block made up the core of the micelles, the soluble B and A blocks apparently formed a mixed corona. Addition of water, a selective solvent for the A block only, caused the B block to become less soluble or insoluble. This increased attraction between the B block, causing the surface B and A chains to shuffle their positions at f_w = 2.9% and f_w = 4.8%. Eventually this led to folding of the cylinder to facilitate aggregations of the B chains. Aging the solvent mixtures at f_w = 7.4% and 10.7% yielded cylinders consisting mainly of segmented stacks of B and C disks. At f_w = 16.7%, the C block in the core mainly formed a fused horseshoe phase. Thicker cylinders with various C and B segregation patterns in the core were observed at f_w = 23%. Aside from these long-term structures, the morphological transitions of the BCA cylinders after water addition were monitored by TEM analysis of samples sprayed at different times after water addition to f_w = 4.8% and 10.7%. Evidently, the cylinders underwent bending more rapidly after water addition to f_w = 10.7%. Some possible mechanisms were proposed to account for the observed intermediates.

IV. Experimental procedures

Materials

Inhibitor-free tetrahydrofuran (THF) purchased from Fisher Scientific was refluxed with sodium and a small amount of benzophenone until a deep purple color developed, and the solvent was then distilled. Diiodomethane (99%) and a 1.4 M solution of *sec*-butyllithium in cyclohexane were purchased from Aldrich. Anhydrous methanol was purchased from Fisher Scientific and was used as received. Pyridine (Aldrich, ≥99%) was refluxed over calcium hydride (Aldrich, reagent grade, 95%) overnight and distilled prior to use. Triethylamine (Aldrich, ≥99%) was refluxed with *p*-toluenesulfonyl chloride (Fluka, ≥99%) and distilled prior to use.

BCA preparation

The precursor to this copolymer was prepared by sequential anionic polymerization of tBA, 2-trimethylsiloxyethyl methacrylate (HEMA–TMS), and DMAEMA. Since the anionic polymerization of tBA and HEMA–TMS has been reported by us in the past[27,34,35] and the anionic polymerization of DMAEMA has been reported by Chen *et al.*,[36] the procedures for the polymerization and monomer purification are not repeated here in any detail.

The anionic polymerization was carried out in THF at −78 °C, and was terminated by the addition of degassed methanol. Stirring the triblock copolymer in THF/methanol/water (v/v/v = 75/24/1) overnight removed the trimethylsiloxy protecting groups to yield poly(2-hydroxyethyl methacrylate), or the PHEMA block. The polymer solution was then concentrated by rotary evaporation and added into excess hexane to precipitate the polymer.

The PHEMA block of the triblock copolymer was converted to PCEMA by reacting the hydroxyl groups with 2 molar equivalents of cinnamoyl chloride in dry pyridine at room temperature in the presence of 2 molar equivalents of triethylamine. After it was stirred overnight, the reaction solution was centrifuged at 2880 rpm (1550*g*) for 6 min to precipitate the salt. The supernatant was dialyzed against methanol in a dialysis tube with a molar mass cutoff of 12 000–14 000 g mol^{-1} in order to remove small-molecular impurities. The methanol was changed 8 times over 48 h. Finally, the targeted copolymer was obtained by precipitation from hexane.

ACB characterization

^{1}H NMR analysis of this sample was recorded on a Bruker 400 MHz spectrometer, using $CDCl_3$ as a solvent. The repeat unit number ratios *l*/*m*/*n* were determined by comparing the ^{1}H NMR integrations corresponding to the three blocks of the copolymer, 1.18/1.00/0.69. The differences between the refractive indices Δn_r of a series of polymer solutions with concentrations between ~3 mg mL^{-1} and ~20 mg mL^{-1} and THF were determined using a Wyatt Optilab rEX refractive index detector. The specific refractive index increment dn_r/dc was obtained from the slope of a Δn_r *vs.* c plot and calculated as 0.119 mL g^{-1}. The number-average molecular weight and polydispersity indices of the samples were determined to be 7.0 × 10^4 g mol^{-1} and 1.05, respectively, by a size-exclusion chromatograph (SEC) equipped with a Wyatt refractive index detector and a Wyatt Dawn Heleos-II light scattering detector. Thus, the number-average repeat unit numbers l, m, and n for the B, C, and A blocks were 160, 135, and 95, respectively.

Micelles

Cylindrical micelles of BCA were prepared by stirring the polymer in methanol at 1.0 mg mL^{-1} between 4 and 7 d. To induce morphological transitions, water was added into the cylindrical micelles within 1 min to a final water volume fraction (f_w) of 2.9%, 4.8%, 7.4%, 10.7%, 16.7%, and 23%.

View Article Online

Published on 04 January 2012. Downloaded by KYUSHU UNIVERSITY on 31/03/2014 01:23:40.

TEM and AFM studies

Aggregates in methanol or water/methanol mixtures were aero-sprayed onto nitrocellulose-coated copper grids using a home-built device.[21] Using this method, most of the methanol had evaporated before the spray hit the coating substrates and water evaporated within 3 s after the spray had landed on the substrates. The samples were further dried at room temperature for 2 h before they were stained by OsO_4 vapor for 2 h for observation by TEM. TEM images were obtained on a Hitachi-7000 instrument operated at 75 kV.

AFM specimens were prepared analogously, except that the TEM grids were replaced with silicon wafers and the staining step was skipped. All samples were analyzed by tapping-mode using a Veeco multimode instrument equipped with a Nanoscope IIIa controller. The tips used were of the Nanosensors™ NCHR-SPL type with a tip radius of ~5 nm. The images were obtained using a free tip oscillation amplitude (A_0) of 60 nm and a set point amplitude ratio (R_{sp}) of ~85%.

TEM tomography

The sample for TEM tomography was aero-sprayed from methanol/water at $f_w = 16.7\%$. Before shipping from Canada to Japan, the sample was irradiated with UV light to crosslink it and stained with OsO_4 vapor to stain the PCEMA domains. For electron tomography, 10 nm Au colloidal solution (GCN005, BBInternational Ltd., UK) was placed on a TEM grid containing the micelles. TEM tomography analysis was done using a JEM-2200FS (JEOL Co. Ltd., Japan) instrument operated at 200 kV. Only the transmitted and elastically scattered electrons with energy loss between 0 and ±15 eV were used for imaging. The images or projections were collected at sample tilting angles ranging from −71° to 77° at 1° intervals. The series of images were aligned by the fiducial marker method[37] using the Au particles. The 3-D images were reconstructed based on the filtered back projection method.[38]

Derivatization of the aggregates

To determine the locations of the A and B chains in the original cylindrical micelles and in the folded cylinder, these blocks were chemically derivatized. This involved first the photolysis of the cylindrical micelles formed in methanol and the folded cylinders formed in methanol/water at $f_w = 4.8\%$ to obtain PCEMA double bond conversions of 62% and 60%, respectively.[27] To stain the PDMAEMA domains in the crosslinked cylindrical micelles in methanol, CH_3I at a molar ratio of 80/1 relative to the DMAEMA units was reacted with the micelles overnight at room temperature.[29] The reaction mixture was subsequently dialyzed against methanol to remove excess CH_3I. The final mixture was concentrated and added into hexane to precipitate the nanofibers. The nanofibers bearing quaternized PDMAEMA units were redispersed into *N*,*N*-dimethylformamide (DMF) before being sprayed for TEM analysis.

The PtBA block was hydrolyzed and the resultant PAA chains were subsequently stained with $UO_2(Ac)_2$ to back-track the location of the original PtBA chains in the crosslinked and folded cylinders. The hydrolysis involved firstly solvent switching from methanol/water to methanol and then to dichloromethane *via* dialysis. PtBA was hydrolyzed using trifluoroacetic acid as the catalyst following previously reported procedures.[35,39] The resultant sample was dialyzed against methanol to remove impurities before it was sprayed onto cellulose-covered TEM grids. Staining was achieved by dispensing one drop of $UO_2(Ac)_2$ that was dissolved in a water/methanol mixture (9/1 v/v) at 20 mg mL^{-1} onto a grid and equilibrating this droplet with a specimen for half an hour before the staining droplet was wicked off with filter paper and the grids were rinsed several times with water droplets.

Solubility of PtBA in methanol/water

A PtBA homopolymer with $M_n = 1.7 \times 10^4$ g mol^{-1} and $M_w/M_n = 1.04$ was dissolved in methanol at 1.0 mg mL^{-1}. Water was subsequently added slowly to 2.00 mL of this solution. After 0.120 mL of water was added, the solution became turbid. The turbidity point for this polymer at this concentration was thus $f_w = 5.7\%$.

Acknowledgements

NSERC of Canada is thanked for sponsoring this research. GL also thanks the Canada Research Chairs Program for a Tier I Canada Research Position in Materials Science.

References

1 G. Wang, X. Tong and Y. Zhao, *Macromolecules*, 2004, **37**, 8911.
2 S. E. Burke and A. Eisenberg, *Langmuir*, 2001, **17**, 6705.
3 S. E. Burke and A. Eisenberg, *Polymer*, 2001, **42**, 9111.
4 L. F. Zhang and A. Eisenberg, *Macromolecules*, 1999, **32**, 2239.
5 Z. J. Hu, A. M. Jonas, S. K. Varshney and J. F. Gohy, *J. Am. Chem. Soc.*, 2005, **127**, 6526.
6 G. Njikang, G. J. Liu and S. A. Curda, *Macromolecules*, 2008, **41**, 5697.
7 G. Njikang, G. J. Liu and L. Z. Hong, *Langmuir*, 2011, **27**, 7176.
8 J. Raez, J. P. Tomba, I. Manners and M. A. Winnik, *J. Am. Chem. Soc.*, 2003, **125**, 9546.
9 F. T. Liu and A. Eisenberg, *J. Am. Chem. Soc.*, 2003, **125**, 15059.
10 H. W. Shen, L. F. Zhang and A. Eisenberg, *J. Am. Chem. Soc.*, 1999, **121**, 2728.
11 J. Rodriguez-Hernandez and S. Lecommandoux, *J. Am. Chem. Soc.*, 2005, **127**, 2026.
12 L. Xu, Z. C. Zhu, O. V. Borisov, E. B. Zhulina and S. A. Sukhishvili, *Phys. Rev. Lett.*, 2009, **103**, 118301.
13 L. F. Zhang, K. Yu and A. Eisenberg, *Science*, 1996, **272**, 1777.
14 B. B. Hong, F. Qiu, H. D. Zhang and Y. L. Yang, *J. Chem. Phys.*, 2010, **132**, 244901.
15 G. L. Hou, L. Zhu, D. Y. Chen and M. Jiang, *Macromolecules*, 2007, **40**, 2134.
16 D. Wang, T. Wu, X. J. Wan, X. F. Wang and S. Y. Liu, *Langmuir*, 2007, **23**, 11866.
17 M. Oba, K. Aoyagi, K. Miyata, Y. Matsumoto, K. Itaka, N. Nishiyama, Y. Yarnasaki, H. Koyama and K. Kataoka, *Mol. Pharmaceutics*, 2008, **5**, 1080.
18 M. H. Li and P. Keller, *Soft Matter*, 2009, **5**, 927.
19 J. M. Hu and S. Y. Liu, *Macromolecules*, 2010, **43**, 8315.
20 Y. Geng, F. Ahmed, N. Bhasin and D. E. Discher, *J. Phys. Chem. B*, 2005, **109**, 3772.
21 J. F. Ding and G. J. Liu, *Macromolecules*, 1999, **32**, 8413.
22 J. Dupont, G. J. Liu, K. Niihara, R. Kimoto and H. Jinnai, *Angew. Chem., Int. Ed.*, 2009, **48**, 6144.
23 X. H. Yan, G. J. Liu, J. W. Hu and C. G. Willson, *Macromolecules*, 2006, **39**, 1906.
24 J. W. Hu, G. Njikang and G. J. Liu, *Macromolecules*, 2008, **41**, 7993.
25 G. J. Liu, J. F. Ding, T. Hashimoto, K. Kimishima, F. M. Winnik and S. Nigam, *Chem. Mater.*, 1999, **11**, 2233.

 This journal is © The Royal Society of Chemistry 2012

View Article Online

26 C. Slim, Y. Tran, M. M. Chehimi, N. Garraud, J. P. Roger, C. Combellas and F. Kanoufi, *Chem. Mater.*, 2008, **20**, 6677.
27 A. Guo, G. J. Liu and J. Tao, *Macromolecules*, 1996, **29**, 2487.
28 G. J. Liu, L. J. Qiao and A. Guo, *Macromolecules*, 1996, **29**, 5508.
29 J. F. Gohy, S. Creutz, M. Garcia, B. Mahltig, M. Stamm and R. Jerome, *Macromolecules*, 2000, **33**, 6378.
30 H. Zhao, Q. J. Chen, L. Z. Hong, L. Zhao, J. F. Wang and C. Wu, *Macromol. Chem. Phys.*, 2011, **212**, 663.
31 G. Battaglia and A. J. Ryan, *J. Am. Chem. Soc.*, 2005, **127**, 8757.
32 S. Jain and F. S. Bates, *Macromolecules*, 2004, **37**, 1511.
33 S. Jain and F. S. Bates, *Science*, 2003, **300**, 460.
34 G. J. Liu, X. H. Yan, Z. Li, J. Y. Zhou and S. Duncan, *J. Am. Chem. Soc.*, 2003, **125**, 14039.
35 X. H. Yan, G. J. Liu and Z. Li, *J. Am. Chem. Soc.*, 2004, **126**, 10059.
36 S. C. Chen, S. W. Kuo, C. S. Liao and F. C. Chang, *Macromolecules*, 2008, **41**, 8865.
37 R. A. Crowther, D. J. Derosier and A. Klug, *Proc. R. Soc. London, Ser. A*, 1970, **317**, 319.
38 H. Jinnai, R. J. Spontak and T. Nishi, *Macromolecules*, 2010, **43**, 1675.
39 X. H. Yan, G. J. Liu, M. Haeussler and B. Z. Tang, *Chem. Mater.*, 2005, **17**, 6053.

Published on 04 January 2012. Downloaded by KYUSHU UNIVERSITY on 31/03/2014 01:23:40.